Use of Aromatase (CYP19) Metabolite Ratios To Characterize Electron Transfer from NADPH–Cytochrome P450 Reductase†

J. Grogan,‡ M. Shou,‡ D. Zhou,§ S. Chen,§ and K. R. Korzekwa*,‡

National Institutes of Health, Bethesda, Maryland 20892, and Beckman Research Institute, Duarte, California 91010

Received May 27, 1993; Revised Manuscript Received August 12, 1993⊕

ABSTRACT: Aromatase catalyzes the conversion of 4-androstene-3,17-dione to estrogen with the concomitant formation of the minor metabolites 4-androstene-19-hydroxy-3,17-dione (19-hydroxyandrostenedione) and 4-androstene-3,17,19-trione (19-oxoandrostenedione). Microsomes of chinese hamster ovary (CHO) cells expressing human aromatase were isolated to investigate androstenedione metabolism. Relatively greater amounts of the minor metabolites result after limitation of electron flux from NADPH–cytochrome P450 reductase to aromatase. Substitution of NADH for NADPH or limitation of NADPH availability increased minor metabolite formation relative to estrogen formation. Similar changes in metabolite ratios were observed when metabolism was conducted either at high pH (8.3) or in the presence of *n*-alcohols in the range of 5–200 mM alcohol concentrations. However, conditions of low pH (5.5) or high ionic strength (1 M KCl) resulted in minor changes in metabolite ratios, suggesting little or no effect on electron flux between NADPH–cytochrome P450 reductase and aromatase. Theoretical molar ratios of the resulting metabolites were predicted using a reaction scheme assuming sequential substrate oxidations without reversible intermediate release from the aromatase active site. This model was supported by a close agreement between theoretical and experimental metabolite ratios for a broad range of NADPH concentrations. The results indicate that metabolite ratios provide a sensitive indicator of aromatase–oxidoreductase interactions in the microsomal environment.

Aromatase is a cytochrome P450 (P450) enzyme that catalyzes the oxidation of androstenedione to estrogen. Interest in specific inhibitors of the enzyme is high due to their possible use in developing treatments for breast cancers and benign prostate hyperplasia (Banting et al., 1989). Tumors regulated by estrogen levels may be treated by inhibition of aromatase, reducing the production and secretion of the hormone. NADPH–cytochrome P450 reductase (oxidoreductase) is a necessary element of the P450 catalytic cycle, transferring electrons to the heme resulting in oxygen activation. Typically, two electrons from oxidoreductase are required for substrate oxidation and product release by P450 enzymes. What is exceptional about the interaction of aromatase with androstenedione is that three sequential substrate oxidations requiring the transfer of six electrons from oxidoreductase are necessary for estrogen formation.

Few generalizations have emerged regarding the interaction between cytochrome P450 and oxidoreductase. The ratio of P450 to oxidoreductase in the microsomal membrane is estimated to be 20:1 (Peterson, 1986). This finding and studies of P450 "aggregates" have suggested that clusters of P450 enzymes interacting with individual or sequestered monomers of oxidoreductase form the effective unit of electron transfer (Franklin & Estabrook, 1971; French et al., 1980; Dean & Gray, 1982). However, rotational diffusion measurements have suggested cytochrome P450 is primarily in an unassociated (mobile) condition at ratios of P450 to oxidoreductase as high as 5:1 (Gut et al., 1982). It has also been shown that the maximum catalytic activity of the major phenobarbital-induced form of P450 from rats occurs at 1:1 ratios of P450 to oxidoreductase in a reconstituted system (Miwa et al., 1979).

The chemical nature of the interaction of P450 and oxidoreductase is also not well defined. Electrostatic interactions resulting in charge pairs may be necessary for the interaction of P450s with oxidoreductase. This has been shown by experiments designed to disrupt such interactions by chemical modification of charged residues or by changes in ambient conditions of charged residue solvation (Tamburini & Schenkman, 1986; Strobel et al., 1989). However, Voznesensky and Schenkman (1992) have suggested that charge repulsion may decrease the stability of oxidoreductase–cytochrome P450 2B4 complexes. They suggest that hydrophobic interactions, possibly occurring through the interaction of membrane-spanning domains, may be important.

The catalytic cycle of aromatase may have special utility in the study of cytochrome P450–oxidoreductase interactions. In the course of estrogen formation by aromatase, androgens are oxidized to the 19-hydroxy and 19-oxo androgen intermediates. In the presence of saturating substrate, estrogen formation occurs when the intermediates are not released from the active site (Thompson & Siiteri, 1974). However, under certain conditions, androgen intermediates are released from the active site prior to estrogen formation, and further oxidation is prevented by saturating androstenedione concentrations. The observation that the extent of intermediate formation depends on the prevailing ratio of aromatase to oxidoreductase led to the suggestion that the interaction of aromatase and oxidoreductase occurs by sequential and independent couplings (Sethumadhavan & Bellino, 1991). The accumulation of minor metabolites may therefore also provide a useful probe of electron flux from oxidoreductase to aromatase. We have investigated metabolite ratios of aromatase under conditions known to result in inefficient electron transfer and have identified metabolite ratios that suggest inefficient reduction of aromatase by oxidoreductase.

† S.C. and D.Z. are supported by NIH Grant CA44735.

* Author to whom correspondence should be addressed at Bldg. 37, Rm. 3E24, National Institutes of Health, Bethesda, MD 20892.

‡ NIH.

§ Beckman Research Institute.

⊕ Abstract published in *Advance ACS Abstracts,* October 15, 1993.

0006-2960/93/0432-12007$04.00/0

EXPERIMENTAL PROCEDURES

Aromatase Expression in CHO Cells. Chinese hamster ovary (CHO) cells stably expressing aromatase were prepared and cultured as described (Zhou et al., 1990). Cells were stored at −80 °C until thawing for the preparation of CHO microsomes. CHO microsomes were prepared by sonication and differential centrifugation. Sonicated cells were centrifuged at 10000*g* for 15 min to obtain a particulate-free supernatant. This material was centrifuged at 100000*g* for 1 h to obtain the pelleted microsomal fraction. Microsomal pellets were resuspended in two pellet volumes of 50 mM potassium phosphate, pH 7.4, and 0.1 M KCl, resulting in suspensions containing 30 mg/mL protein by the bicinchoninic acid method (Pierce). Total aromatase activity recovered by this procedure was 60–80% of that in whole cell suspensions used directly after sonication.

Incubation Conditions and Metabolite Analysis. Microsomal suspensions were added into 50 mM potassium phosphate buffer at pH 7.4, resulting in a final protein concentration of 0.3 mg/mL microsomal protein. Incubations were otherwise prepared as described (Zhou et al., 1992), with the exception that 50 μM progesterone was not included in the incubations. The 5-α-reductase activity was negligible under the conditions of these assays. Total substrate conversion was between 5% and 20%. Incubation buffer for experiments investigating the differences in metabolism due to buffer pH were prepared first by adjusting the pH of 100 mM sodium pyrophosphate buffer to the desired pH value (pyrophosphate buffer was used for this experiment because of its wide buffering range). The conductance of solutions was then adjusted with saturated sodium chloride solutions to 23 ± 2 mmho. The resulting solutions were analyzed for pH prior to addition of the microsomal suspension and the remaining reaction components. These additions did not significantly change solution pH values. Experiments involving alcohol in the incubations were prepared by addition of 0.5 M alcohol stock solutions into 50 mM potassium phosphate buffer at pH 7.4 prior to addition of microsomal suspension. After 5 min at room temperature, reactions were initiated by substrate and NADPH additions.

Incubations at 37 °C were terminated after 20 min by the addition of 2.5 mL of dichloromethane. Products were analyzed by HPLC and radioactive metabolite detection as previously described (Zhou et al., 1992). No metabolites were observed for incubations without cofactor. Metabolites other than estrogen, 19-hydroxyandrostenedione, and 19-oxoandrostenedione were not observed under the conditions of this assay.

Metabolite mole fractions were defined by the ratios of the individual metabolites to the sum of all metabolites measured by peak integration of radioactivity in the HPLC effluent. The values of the metabolite mole fractions in control incubations were not significantly changed for incubations terminated after 5–30 min. Theoretical iterative curve fits to the experimental data for NADPH limitation were obtained using Kaleidagraph (Abelbeck Software). Intitial fits were obtained for the metabolite mole fraction of 19-hydroxyandrostenedione, and the resulting constants (k_{31} and k_R) were fixed for subsequent curve fitting of the metabolite mole fractions of 19-oxoandrostenedione and estrogen.

Materials. NADPH and NADH were from Boehringer Mannheim. NADH was separated from contaminating NADPH immediately prior to incubations. Briefly, a 20 mM solution of NADH was loaded onto a 5/5 Mono Q column (Pharmacia) and eluted with a linear gradient from 10 mM potassium phosphate to 0.2 M NaCl and 0.2M potassium phosphate at pH 7.4. The concentration of NADH collected was estimated using absorbance at 254 nm. [7-^{3}H]Androst-4-ene-3,17-dione at a specific activity of 18.50 Ci/mmol was obtained from New England Nuclear. Unlabeled steroid standards were obtained from Steraloids. All other chemicals were of analytical grade.

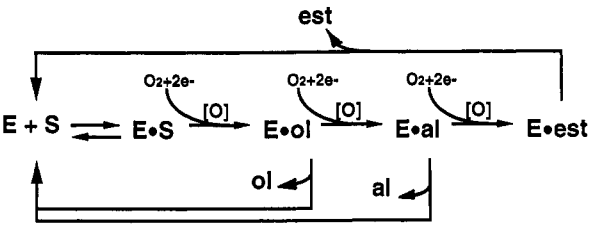

FIGURE 1: Metabolism of androstenedione (S) to estrogen (est) by aromatase (E). Minor metabolites are 19-hydroxyandrostenedione (ol) and 19-oxoandrostenedione (al). Oxidation steps requiring oxygen, NADPH, and NADPH–cytochrome P450 reductase are designated by [O].

Table I: Effect of Cofactor Substitution on Aromatase Metabolism[a]

cofactor	% control activity	X_m [std dev][b] (n = 4) ol	al	est
NADPH	100	0.15 [0.01]	0.05 [0.01]	0.80 [0.02]
NADH	43	0.24 [0.01]	0.17 [0.01]	0.59 [0.02]
NADH/NADPH ratio[c]	na	1.6	3.4	0.7

[a] Metabolism of [7-^{3}H]androstenedione by microsomes from CHO cells expressing human aromatase. Cofactor concentrations in the incubations were 1 mM NADH or NADPH, with other conditions as described in Experimental Procedures. Percent control activity is the substrate metabolized expressed as a percent of substrate metabolized in incubations with 1 mM NADPH cofactor at pH 7.4. [b] Metabolite mole fractions (X_m) represent the radioactivity of individual metabolites divided by the sum of radioactivity recovered for all metabolites. "ol" represents 19-hydroxyandrostenedione, "al" represents 19-oxoandrostenedione, and "est" represents estrogen. [c] Ratio of mole fraction of the individual metabolites obtained with NADH as cofactor divided by the mole fraction obtained with NADPH as cofactor. na, not applicable.

RESULTS

The metabolism of androstenedione by aromatase is represented in the simplified reaction scheme shown in Figure 1. The minor metabolites, 19-hydroxyandrostenedione (ol) and 19-oxoandrostenedione (al) represent intermediates which dissociate from the enzyme–substrate complex prior to estrogen formation. Estrogen (est), the final metabolite, is formed when dissociation does not occur. The catalytic oxidations ([O] in Figure 1) are complex, each representing oxygen binding, oxygen activation, and substrate oxidation. Oxygen activation requires electron transfer reactions involving the coenzymes NADPH, FMN, and FAD. The catalytic oxidations also must involve the physical association of aromatase and oxidoreductase. We reasoned that if the formation of estrogen is dependent upon the efficiency of electron transfer, the effect of slowing the rate of aromatase reduction will be to decrease the estrogen formed relative to the sum of all metabolites. We have first established this dependence using oxidoreductase cofactor substitution to restrict electron flux from oxidoreductase to aromatase.

Table I shows the effects of substituting the less effective cofactor, NADH, for NADPH in the assay of aromatase metabolites. The androstenedione consumption by aromatase decreases 57% in incubations containing NADH relative to those with NADPH (see % control activity, Table I). We

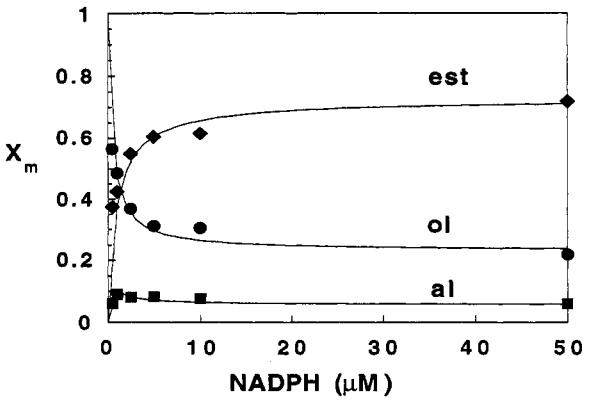

FIGURE 2: Experimental and theoretical metabolite mole fractions. The data points represent the individual metabolite mole fractions of 19-hydroxyandrostenedione (●), 19-oxoandrostenedione (■), and estrogen (◆) at the NADPH concentrations indicated. Metabolite mole fractions (X_m, ordinate) were determined as described in the legend of Table I and Experimental Procedures. The lines shown represent the theoretical fits obtained using the equations described in Table II.

attribute this decrease to the higher K_m of oxidoreductase for NADH relative to NADPH (Milewich et al., 1981b; Sheean & Meigs, 1983). The fractions of each metabolite formed as a function of the sum of all metabolites are also presented in Table I (see X_m, the metabolite mole fraction). In the presence of NADH the relative amounts of 19-oxygenated metabolites formed increases, while estrogen decreases.

Another method of restricting electron flux between oxidoreductase and aromatase is limitation of cofactor availability. Total metabolism decreases gradually as NADPH in the incubations is limited from 50 to 5 μM cofactor. At concentrations less than 5 μM NADPH, total metabolism shows a greater dependence on cofactor concentration. Double-reciprocal analysis of the rate data gave an apparent K_m of 2 μM for NADPH. The decrease in total androstenedione metabolism is reflected by the amount of estrogen formed as a function of all metabolites as shown in Figure 2. The mole fraction of estrogen formed at 50 μM NADPH (Figure 2, $X_m = 0.72$) is gradually lessened as NADPH concentration is reduced to 5 μM. At cofactor concentrations less than 5 μM NADPH, the estrogen mole fraction decreases dramatically to a value of 0.37 at 0.5 μM NADPH. In contrast, the dependence of the minor metabolite mole fractions on cofactor concentration are strikingly different from those of estrogen. The mole fraction of 19-hydroxyandrostenedione increases gradually as cofactor is limited to 5 μM NADPH concentration and then increases sharply at less than 2.5 μM cofactor concentration, in an inverse relation to changes in estrogen mole fractions. The cofactor concentration dependence of the 19-oxoandrostenedione mole fraction is more complex, increasing gradually as cofactor is limited, before decreasing sharply at less than 2.5 μM cofactor concentration.

We were interested in fitting the data of Figure 2 to a kinetic model based on the aromatase reaction scheme (Figure 1). A schematic method (King & Altman, 1956) was used to derive the kinetic equations for the aromatase reaction scheme shown in Figure 3. We have simplified the reaction scheme and resulting kinetic constants by assuming that estrogen formation is accompanied by fast release (Osawa, 1973). This is represented by the parallel arrows from enzyme–19-oxoandrostenedione intermediate (E-al) to free enzyme (E). The rate constant k_{45} in this reaction scheme describes a single rate representing the conversion of E-al to estrogen and free enzyme. The rate constant k_{41} represents

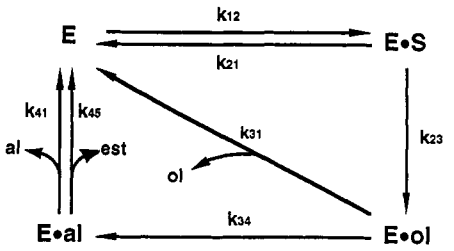

FIGURE 3: Kinetic reaction scheme utilized for determination of velocity equations. The reactions depicted in Figure 1 were used to derive the relation of free enzyme and intermediates using the method of King and Altman (1956). The double arrow shown between E•al and E is discussed in the text. k_{45} describes the rate of enzyme–19-oxoandrostenedione conversion to enzyme–estrogen intermediate. Subsequent release of estrogen from the enzyme–estrogen intermediate is assumed to be rapid and is ignored.

the dissociation of the aldehyde intermediate from E-al precluding further oxidation of substrate by aromatase. The rate constants k_{23}, k_{34}, and k_{45} are for reactions involving reductase and oxygen, while the constants k_{31} and k_{41} represent enzyme–intermediate dissociation reactions. The resulting constants were used to derive the velocity ratios shown in Table II (column 2). Simplification of the velocity ratios results when the three oxidation rates ($k_{23} = k_{34} = k_{45}$) are assumed to be dependent upon three equivalent reduction rates. Under these conditions the velocity ratios for rates of metabolites formed are greatly simplified and include just three variables: k_{31}, k_{41}, and k_R (Table II, column 3). To describe the effects of subsaturating NADPH concentrations, k_R can be replaced by the standard Michaelis–Menten relationship: $k_R = V_{max}[NADPH]/(K_m + [NADPH])$. Thus, the velocity ratios could be described by the relative values of V_{max} (reduction) and the off-rate constants k_{31} and k_{41}. The resulting kinetic expressions were used as a basis for fitting theoretical curves to the experimental data shown in Figure 2.

The best fit of these equations to the experimental data in Figure 2 is obtained with a ratio of the intermediate dissociation rate constants of $k_{41}/k_{31} = 0.27$ and a ratio of V_{max}/k_{31} of 3.24. The theoretical curves obtained using this ratio of dissociation rate constants results in the curves shown over the experimental data points in Figure 2. The fit of the theoretical predictions of metabolite mole fractions is in excellent agreement with the experimental results obtained by cofactor limitation, even for the unusual behavior of the aldehyde intermediate. We have used this result as a basis for investigation of changes in electron flux resulting from conditions that reduce total aromatase activity. These conditions include incubation at high and low pH and incubations in the presence of *n*-alcohols.

The pH–activity profile of aromatase is shown in Figure 4, panel A. A pH maximum of pH 6.5–7.5 is observed together with a broad pH–activity profile spanning 3 pH units. As much as 22% of maximum activity (pH 7 = 100%) is observed at pH 5.5, with 28% of maximum activity at pH 8.3. Figure 4, panel B shows the values of metabolite mole fractions as a function of pH at the percent of maximum activity indicated in Figure 4, panel A. The individual mole fractions at low pH values, less than about pH 7, are similar to those obtained at the pH maximum. However, at pH values greater than 7, 19-hydroxyandrostenedione and 19-oxoandrostenedione mole fractions increase at the expense of estrogen metabolite mole fractions. These effects on metabolite mole fractions are most pronounced at pH 8.3, where 19-hydroxyandrostenedione and 19-oxoandrostenedione represent greater than 50% of total

Table II: Theoretical Kinetic Expressions for Metabolite Formation[a]

velocity ratio	velocity ratios derived from kinetic scheme: model	$k_R = k_{23}, k_{34}, k_{45}$
$V_{ol}/(V_{ol} + V_{al} + V_{est})$	$(k_{41} + k_{45})k_{23}k_{31}/[k_{31}k_{23}(k_{41} + k_{45}) + k_{23}k_{34}k_{41} + k_{23}k_{34}k_{45}]$	$k_{31}/(k_{31} + k_R)$
$V_{al}/(V_{ol} + V_{al} + V_{est})$	$k_{23}k_{34}k_{41}/[k_{31}k_{23}(k_{41} + k_{45}) + k_{23}k_{34}k_{41} + k_{23}k_{34}k_{45}]$	$k_{41}/[(k_{31}k_{41}/k_R) + k_{31} + k_{41} + k_R]$
$V_{est}/(V_{ol} + V_{al} + V_{est})$	$k_{23}k_{34}k_{45}/[k_{31}k_{23}(k_{41} + k_{45}) + k_{23}k_{34}k_{41} + k_{23}k_{34}k_{45}]$	$k_R/[(k_{31}k_{41}/k_R) + k_{31} + k_{41} + k_R]$

[a] Velocity ratios were derived using the kinetic scheme shown in Figure 3, using the method of King and Altman (1956). Velocities of 19-hydroxyandrostenedione (V_{ol}), 19-oxoandrostenedione (V_{al}) and estrogen (V_{est}) formation were substituted into the velocity ratio expressions to yield the "model" ratios given. The resulting expressions were simplified by assuming all reduction rate constants were equivalent ($k_R = k_{23},k_{34},k_{45}$). These expressions were used after accounting for (1) saturation of the reduction rate [i.e., $k_R = (V_m[NADPH])/(K_m + [NADPH])$] and (2) the apparent inequivalence of the off-rate constants, k_{31} and k_{41}, as discussed in the text. The resulting fit of these equations to the experimentally determined metabolite mole fractions are represented by solid lines in Figure 2.

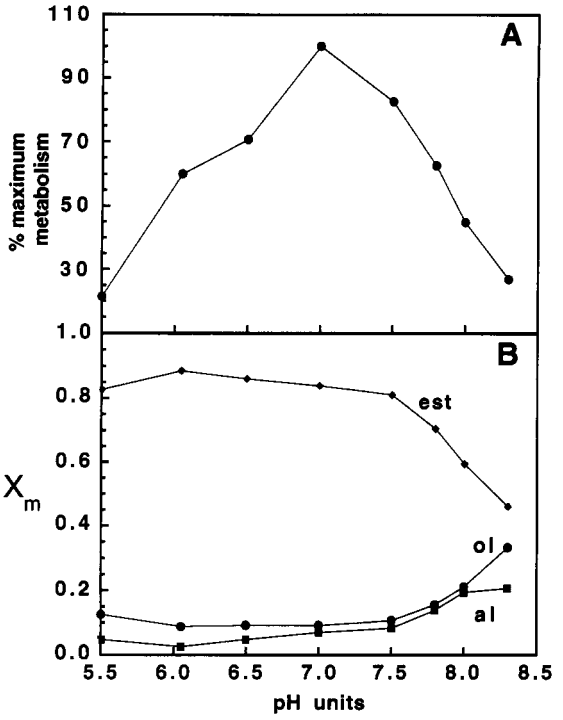

FIGURE 4: Influence of incubation pH on metabolite formation. Reaction incubations were conducted in 100 mM pyrophosphate buffer at pH values in the range of 5.5–8.3. Panel A shows total aromatase metabolism resulting after analysis as described in Experimental Procedures at the pH values indicated on the ordinate scale (panel B). Percent maximum activity is total androstenedione metabolism normalized to activity at pH 7 (pH 7 = 100%). Metabolite mole fractions (X_m) are shown in panel B for the corresponding values of percent maximum activity shown in panel A. The symbols represent 19-hydroxyandrostenedione (●), 19-oxoandrostenedione (■), and estrogen (◆).

metabolite formation. This is in contrast to results obtained at pH values less than 7. The intermediate metabolites together represent less than 20% of total metabolite formation in this lower pH range. The metabolite mole fractions at high pH values, above 7.5, are similar to those observed upon limitation of cofactor availability (Figure 2; in the range of 0.5–5.0 μM NADPH concentration).

1-Alkanols are known to affect membrane order. 1-Alkanols with short alkyl chains have a relatively greater effect on membrane disorder than those with longer alkyl chains (Miller et al., 1989). The effect of alcohols on aromatase activity may therefore provide a means of investigating the influence of membrane structural features on aromatase–oxidoreductase interactions. Table III shows that aromatase activity is inhibited in the range of 5–200 mM alcohol concentrations. Octanol inhibits activity at lower concentrations than butanol (Table III; compare 32 mM octanol and 50 mM butanol). The trends in metabolite mole fractions at the alcohol

Table III: Effect of Alcohols on Aromatase Metabolism[a]

incubation condition: alcohol	alcohol concn (mM)	% control activity	X_m: ol	al	est
none (control)	0	100	0.147	0.052	0.801
butanol	20	113[b]	0.188	0.089	0.724
	50	61	0.262	0.120	0.618
	200	<3	ns	ns	ns
octanol	5	98	0.151	0.075	0.774
	20	9	0.349	0.147	0.504
	32	<1	ns	ns	ns

[a] Incubations were as described in Experimental Procedures at the alcohol concentrations indicated. Percent control activity and metabolite mole fractions (X_m) were calculated as described in the legend of Table I. ns signifies that the metabolite mole fractions could not be estimated reliably from the data. [b] A significant increase in activity was consistently observed over controls in the presence of 20 mM butanol.

Table IV: Michaelis Constants and Metabolite Mole Fractions in the Presence of Inhibitors[a]

incubation conditions	K_m (nM)	% control activity[b]	X_m: ol	al	est
incubation pH					
pH 7.4	7.4	100	0.097	0.077	0.826
pH 5.6	86.8	26	0.140	0.065	0.795
pH 8.3	20.5	32	0.443	0.231	0.326
alcohol					
57 mM butanol	21.8	58	0.153	0.131	0.686
88 mM butanol	38.1	42	0.242	0.176	0.582
111 mM butanol	47.5	26	0.275	0.163	0.562
ionic strength					
0.1 M KCl	nd	87	0.061	0.114	0.829
0.25 M KCl	nd	59	0.074	0.147	0.779
1.00 M KCl	nd	28	0.072	0.205	0.723

[a] Apparent K_m values were estimated using the incubation conditions indicated. Incubations for the given conditions were prepared as described in Experimental Procedures. The correlation coefficients of Lineweaver–Burk analyses were typically greater than 0.99. nd, not determined. [b] The percent of control activity and the metabolite mole fractions given are for incubations at 100 nM substrate concentration as described in the legend of Table I.

concentrations resulting in partial inhibition of metabolism suggest limitations of electron flux similar to those observed for cofactor limitation. At 50 mM butanol concentration, resulting in 61% of control activity, 19-oxygenated metabolites (i.e., ol and al in Table III) represent a greater proportion of all metabolites than is observed for control incubations. A similar result is observed at 20 mM octanol concentration, at which only 9% of control activity remains.

To further investigate the influence of the various inhibitory incubation conditions upon aromatase activity we have measured kinetic parameters. The effects of low pH (pH = 5.6) on the apparent K_m of aromatase is much greater than that resulting from high incubation pH (pH = 8.3) as shown

in Table IV. This is consistent with metabolite mole fractions at high pH reflecting an impaired reduction of aromatase by oxidoreductase. However, the decrease in activity resulting at pH values less than 7.4 suggests a change in substrate affinity of aromatase and not the efficiency of electron transfer from oxidoreductase.

Butanol results in inhibition of aromatase only at relatively high concentrations. As butanol concentration in the incubations is increased from 57 to 111 mM butanol, the K_m increases about 2-fold. The metabolite mole fraction of estrogen is decreased as butanol concentration is increased, while those of the 19-oxygenated intermediates increase proportionally. The influence of ionic strength on aromatase activity and metabolite mole fractions are also presented in Table IV. Only very high KCl concentrations result in significant inhibition of aromatase activity. Metabolite mole fractions under these conditions are very similar to controls. However, an increase in aldehyde formation with increasing ionic strength is apparent.

DISCUSSION

The cytochrome P450 enzymes oxidize a variety of hydrophobic substrates and are responsible for several metabolic conversions of steroids. Substrate oxidation occurring on multiple sites of a substrate is common for cytochrome P450 enzymes; however, aromatase can catalyze multiple sequential oxidations without release of substrate or intermediates from the active site. Proteins which interact with mammalian cytochrome P450 enzymes and influence activity are NADPH–cytochrome P450 reductase (oxidoreductase) and cytochrome b_5. Cytochrome b_5 has been shown to interact with cytochrome P450 enzymes by electrostatic interactions involving carboxyl groups on the proteins' surfaces (Vermilion & Coon, 1978). The interactions of cytochrome P450 enzymes with oxidoreductase are essential for activity, but the nature of these associations is not clearly defined (Tamburini & Schenkman, 1986).

At cofactor concentrations saturating in NADPH, substitution of NADH in incubations results in lower aromatase activiy (Thompson & Siiteri, 1974). The K_m of oxidoreductase for NADH is 1 mM (Milewich et al., 1981b; Sheean & Meigs, 1983), much higher than that for NADPH (see Figure 2; apparent K_m = 2 μM). We also have shown that at subsaturating concentrations NADH supports less total aromatase activity when substituted for NADPH. Table I shows that metabolite mole fractions of the minor metabolites increase in the presence of NADH. The higher value of metabolite mole fractions of the minor metabolites suggests that any means of reducing the electron supply to aromatase may result in similarly altered metabolite ratios. Limitation of NADPH availability is another method of investigating changes in electron flux from oxidoreductase to aromatase. At concentrations of NADPH near its K_m the metabolite mole fraction of 19-hydroxyandrostenedione surpasses the same fraction for that of estrogen.

When developing a kinetic model for the reaction scheme in Figure 1, assumptions were made that oxidation rates were solely dependent on the rates of reduction and that reduction rates for each step were equal ($k_{23} = k_{34} = k_{45}$, in Figure 3). This allowed the relative values of three rate constants, k_{31}, and k_{41} and V_{max}, to be fit to the experimental data in Figure 2. The ratio of k_{31} to k_{41} of 0.27 provided the best fit for the observed differences in the amounts of alcohol and aldehyde. The ratio of V_{max} to k_{31} of 3.24 provided the observed maximum estrogen mole fraction of 0.8. This maximum of less than unity suggests that other intrinsic features of CHO microsomes limit the reduction rate. These limiting factors may include protein concentrations or membrane conditions. After incorporation of these terms into our kinetic scheme based on the reactions shown in Figure 1, we obtained good agreement between experimental data and predicted metabolite mole fractions. This agreement reinforces our belief in the validity of the kinetic model of androstenedione metabolism shown in Figure 1 and strongly suggests that reduction by oxidoreductase is rate-limiting.

The results of experiments designed to change electron flux rates suggest that the metabolite mole fractions of aromatase provide a sensitive measure of the effectiveness of electron transfer. However, it is conceivable that an alteration in the rate of electron transfer between oxidoreductase and P450 is not responsible in all cases for observed changes in metabolite ratios. For example, a change in protein conformation that results in decreased binding constants for the intermediates would have an effect similar to that of subsaturating NADPH concentrations in our model. We have therefore investigated kinetic constants to further distinguish between these possibilities (Table IV). Inhibition of activity resulting in altered metabolite ratios and only minor changes in the K_m are considered evidence for impaired electron transfer.

Total aromatase metabolism has been shown to have a broad pH–activity profile with a pH of maximum activity in the range of 7.1–8.0 (Reed & Ohno, 1976; Milewich et al., 1981a; Chikhaoui et al., 1985; Muto & Tan, 1986; Silberzahn et al., 1988). We have also shown a pH–activity relationship with a pH of maximal activity in the range of 7–8 (Figure 4, panel A). What is of special interest is the result shown in Figure 4, panel B, showing the relationship between metabolite mole fractions and pH. Although the mole fractions at the high and low pH extremes yield nearly the same total activity (Figure 4, pH 5.5, 21% of activity at pH 7; pH 8.3, 27% of activity at pH 7), metabolite mole fractions are very different. At high pH values, metabolite mole fractions are similar to those observed under conditions of limited reduction rates (i.e., [NADPH] < 5 μM; Figure 2). At low pH, the metabolite mole fractions are relatively insensitive to changes in pH, resembling those at the pH maximum. This result indicates that reduction of aromatase by oxidoreductase is sensitive to hydrogen ion concentration, particularly at pH values greater than 7. The change in apparent K_m values at high incubation pH (Table IV) is also consistent with the idea that the lower activity observed results from reduced electron flux. Oxidoreductase activity in the absence of membrane lipid (i.e., cytochrome c reduction) occurs with a maximal activity at pH 8.2 (Masters et al., 1967). These results suggest that oxidoreductase function is impaired toward aromatase at pH values above 7.0 in CHO cell microsomes. This sensitivity may result from changes in the ionization state of protein, membrane functional groups, or oxidoreductase cofactor. Changes in the rate of substrate turnover at low pH values, below 7, may result from changes in the interactions of aromatase and substrate rather than changes in electron flux between the proteins. The higher apparent K_m for substrate at low pH values (Table IV) is also consistent with this interpretation.

Similar changes in metabolite mole fractions were observed for inhibition of aromatase by alcohols. Detergents, as well as other incubation conditions affecting membrane order, have been shown to influence cytochrome P450 activity (Wagner et al., 1984). Alcohols are also known to influence membrane order parameters (Miller et al., 1989). Since aromatase and

oxidoreductase interact in the membrane environment, inhibition of aromatase activity may be a result of the effect of alcohols on membrane order. However, since concentrations of alcohols in the millimolar range were required for aromatase inhibition, other explanations are possible for the suggested reduction of electron transfer in the presence of alcohols. In particular, substrate and intermediate partitioning in the aqueous phase may alter aromatase–intermediate dissociation rates, or weakened associations of membrane-excluded domains of aromatase and oxidoreductase may be relevant.

Ionic strength decreases total aromatase metabolism only at relatively high KCl concentrations (Table IV), while little change in metabolite mole fractions is observed. This result indicates that the interaction of aromatase and oxidoreductase is not primarily dependent upon the formation of charge-paired electrostatic interactions. Were such residue charge pairs necessary for aromatase–oxidoreductase electron transfer, metabolite mole fractions would be expected to change sharply as total aromatase activity is decreased. These results for aromatase are therefore consistent with previous findings regarding putative charge-pairing interactions between cytochrome P450 2B4 and oxidoreductase (Voznesensky & Schenkman, 1992).

The unique sequential interactions of aromatase and oxidoreductase may thus provide a useful kinetic approach to investigation of cytochrome P450–oxidoreductase association. Distinguishing between rigid versus nonrigid models for membrane configurations of cytochrome P450 and oxidoreductase enzymes (Peterson et al., 1976; Yang, 1977) may also be investigated using aromatase metabolite ratios. We are currently interested in experiments in which greater control of enzyme concentration is possible to address this question.

REFERENCES

Banting, L., Nicholls, P. J., Shaw, M. A., & Smith, H. J. (1989) *Prog. Med. Chem. 26*, 253.

Chikhaoui, Y., Chitour, F., Boussioux, A. M., Nicolas, J. C., Descomps, B., & Crastes de Paulet, A. (1985) *J. Steroid Biochem. 22*, 727.

Dean, W. L., & Gray, R. D. (1982) *J. Biol. Chem. 257*, 14679.

Franklin, M. R., & Estabrook, R. W. (1971) *Arch. Biochem. Biophys. 143*, 318.

French, J. S., Guengerich, F. P., & Coon, M. J. (1980) *J. Biol. Chem. 255*, 4112.

Gut, J., Richter, C., Cherry, R. J., Winterhalter, K. H., & Kawato, S. (1982) *J. Biol. Chem. 257*, 7030.

King, E. L., & Altman, C. (1956) *J. Chem. Phys. 60*, 1375.

Masters, B. S. S., Williams, C. H., Jr., & Kamin, H. (1967) *Methods Enzymol. 10*, 565.

Milewich, L., Chen, G. T., MacDonald, P. C., & Peterson, J. A. (1981a) *J. Steroid Biochem. 14*, 185.

Milewich, L., Hendricks, T. S., Masters, B. S., Frenkel, R. A., & MacDonald, P. C. (1981b) *Arch. Biochem. Biophys. 211*, 530.

Miller, K. W., Firestone, L. L., Alifimoff, J. K., & Streicher, P. (1989) *Proc. Natl. Acad. Sci. U.S.A. 86*, 1084.

Miwa, G. T., West, S. B., Huang, M., & Lu, A. Y. (1979) *J. Biol. Chem. 254*, 5695.

Muto, N., & Tan, L. (1986) *Biochem. Biophys. Res. Commun. 136*, 454.

Osawa, Y. (1973) in *Endocrinology, Proceedings of the 4th International Congress of Endocrinology* (Scow, R. O., Ed.) pp 814–819, Excerpta Medica, Amsterdam.

Peterson, J. A. (1986) in *Cytochrome P-450: Structure, Mechanism and Biochemistry* (Ortiz de Montellano, P. R., Ed.) pp 89-117, Plenum Press, New York.

Peterson, J. A., Ebel, R. E., O'Keefe, D. H., Matsubara, T., & Estabrook, R. W. (1976) *J. Biol. Chem. 251*, 4010.

Reed, K. C., & Ohno, S. (1976) *J. Biol. Chem. 251*, 1625.

Sethumadhavan, K., & Bellino, F. L. (1991) *J. Steroid Biochem. Mol. Biol. 39*, 381.

Sheean, L. A., & Meigs, R. A. (1983) *Steroids 42*, 77.

Silberzahn, P., Gaillard, J. L., Quincey, D., Dintinger, T., & Al-Timimi, I. (1988) *J. Steroid Biochem. 29*, 119.

Strobel, H. W., Nadler, S. G., & Nelson, D. R. (1989) *Drug Metab. Rev. 20*, 519.

Tamburini, P. P., & Schenkman, J. B. (1986) *Arch. Biochem. Biophys. 245*, 512.

Thompson, E. A., Jr., & Siiteri, P. K. (1974) *J. Biol. Chem. 249*, 5364.

Vermilion, J. L., & Coon, M. J. (1978) *J. Biol. Chem. 253*, 2694.

Voznesensky, A. I., & Schenkman, J. B. (1992) *J. Biol. Chem. 267*, 14669.

Wagner, S. L., Dean, W. L., & Gray, R. D. (1984) *J. Biol. Chem. 259*, 2390.

Yang, C. S. (1977) *Life Sci. 21*, 1047.

Zhou, D., Pompon, D., & Chen, S. (1990) *Cancer Res. 50*, 6949.

Zhou, D., Korzekwa, K. R., Poulos, T., & Chen, S. (1992) *J. Biol. Chem. 267*, 762.